two-carbon backbone ($TcOEn(AO)_2$) the bite angle of the nitrogens is 82.5 (1)°, the nitrogens are deprotonated and planar, and the N–Tc distances are short. Adding a third carbon to the backbone to make a six-membered ring ($TcOPn(AO)_2$) introduces some change, as shown by the increased bite angle (92.7°). However, the nitrogens are still deprotonated and planar and the Tc–N distances remain nearly the same. The five- and six-membered ring systems are able to accommodate the planar nitrogens without much strain. Increasing the backbone size to five carbons gives an eight-membered ring ($TcO_2Pent(AO)_2$). This increased ring size makes it difficult to maintain a small bite angle and short Tc–N distances without considerable puckering of the ring. This same argument must apply to the seven-membered ring system with a four-carbon backbone ($TcO_2Bn(AO)_2$). In the larger ring systems ring strain inhibits deprotonation of the nitrogens by favoring tetrahedral sp^3 nitrogens and long Tc–N distances.

Acknowledgment. The authors wish to thank Dr. R. B. Taylor for his assistance in obtaining the NMR spectra. Financial support by Amersham International (S.J., K.A., D.E.T.) and the National Science Foundation, Grant No. CH#81-06795 (E.O.S.), is gratefully acknowledged. Support toward purchase of the X-ray instrument by NSF Grant No. CHE 7820347 is also acknowledged.

Registry No. $^{99}TcO(AO)_2$, 109959-88-8; $^{99}TcOEn(AO)_2$, 95180-93-1; $^{99}TcO_2Bn(AO)_2$, 109959-89-9; $^{99}TcO_2Pent(AO)_2$, 109959-90-2; $^{99}TcO_2Pent(AO)_2 \cdot 2CHCl_3$, 109959-91-3; $Pent(AO)_2$, 109929-73-9; chloroxime, 3238-16-2; $NH_4{}^{99}TcO_4$, 34035-97-7; $SnC_4H_4O_6$, 815-85-0; 1,5-diaminopentane, 462-94-2.

Supplementary Material Available: Tables of positional parameters for hydrogen atoms, thermal parameters, bond distances and angles, and least-squares planes (13 pages); listings of observed and calculated structure factors (37 pages). Ordering information is given on any current masthead page.

Contribution from the Institut für Physikalische und Theoretische Chemie and Physikalisches Institut, Abt. II, University of Erlangen-Nürnberg, D-8520 Erlangen, West Germany, and Department of Chemistry, The Queen's University of Belfast, Belfast BT9 5AG, Northern Ireland

Detailed Study of a Two-Step Quintet ⇌ Singlet Spin Transition in an Iron(II) Complex with a N_3O_2 Macrocyclic Ligand and the Kinetics of the Quintet → Singlet Relaxation in the Temperature Range 115–130 K

E. König,*[1a] G. Ritter,[1b] J. Dengler,[1b] and S. M. Nelson[2]

Received March 3, 1987

The complicated high-spin (HS, $S = 2$) ⇌ low-spin (LS, $S = 0$) transition in the solid iron(II) complex $[FeL(CN)_2]\cdot H_2O$ of a N_3O_2 macrocyclic Schiff-base ligand L has been studied in detail. When the sample is cooled slowly, a transition from the HS form to a form with approximately equal proportions of HS and LS is observed ($T_c^{\downarrow} = 207$ K). The transition is reversible ($T_c^{\uparrow} = 222$ K) and, due to the pronounced hysteresis of $\Delta T_c = 15$ K, thermodynamically first order. On reasonably fast cooling (10–20 K min^{-1}) from 300 K to temperatures between 150 and 160 K, the HS form is retained but transforms after several minutes into the LS form. The lower the temperature, the greater the LS fraction. The transformation is irreversible and fast, and below ~150 K it is practically complete. On warming of the LS form, a transformation to the HS:LS = 1:1 form is observed at $T_c = 157$ K. If the sample is rapidly quenched to 77 K, the HS form is frozen in, an irreversible transformation to LS setting in if the sample is warmed to above 110 K. The kinetics of the HS → LS relaxation has been investigated between 115.7 and 130.0 K. The rate constant for the process varies between $k = 6.77 \times 10^{-5}$ and 2.31×10^{-3} s^{-1}, the activation energy being $\Delta E = 7.3$ kcal mol^{-1}. In X-ray diffraction, the transformations are characterized by the replacement of individual diffraction patterns, thus establishing that the unit cells of the forms involved are all different. The quadrupole splitting for the LS form ΔE_Q^{LS} is characterized by a significant dependence on t_{HS}/t_{tot} and thus n_{HS}. It is believed that the dependence arises since the HS form is seven-coordinate, while the LS form is six-coordinate with one ether oxygen of the macrocycle uncoordinated.

Introduction

Recently, we have reported[3] on the synthesis and some unusual properties of the iron(II) complex $[FeL(CN)_2]\cdot H_2O$ with the macrocyclic Schiff-base ligand L derived from the condensation of 2,6-diacetylpyridine with 3,6-dioxaoctane-1,8-diamine. Magnetic susceptibilities and the ^{57}Fe Mössbauer effect, which were studied over the temperature range 80–300 K, revealed a complex variation of the ground state with temperature. At ambient temperature, the thermodynamically stable form is high spin (HS), evidence being the effective magnetic moment $\mu_{eff} = 5.09$ μ_B and the Mössbauer spectrum characterized by the quadrupole splitting $\Delta E_Q = 3.18$ mm s^{-1} and the isomer shift $\delta^{IS} = +0.84$ mm s^{-1} at 293 K. When the complex was slowly cooled to 225 K, the magnetic moment started to decrease, its value leveling out below ca. 210 K at 3.58 μ_B. Mössbauer-effect measurements showed that the apparently stable form consists of the high-spin (HS) and low-spin (LS) ground states in an almost equal proportion. The transition is reversible, although the transformation to the pure HS state arises at ca. 220 K, i.e. at a somewhat higher temperature. There is therefore a pronounced hysteresis loop associated with the transition. The HS form may be frozen in if the sample is rapidly cooled in liquid nitrogen. Slow warming of the quenched-in HS complex produced an abrupt decrease of the magnetic moment above ca. 110 K from 5.0 to ~1.00 μ_B. On the basis of the Mössbauer study, the result of this transformation is the practically pure LS state of the complex characterized, at 151.2 K, by the values $\Delta E_Q = 1.43$ mm s^{-1} and $\delta^{IS} = +0.28$ mm s^{-1}. If the sample is now slowly warmed up, first a transformation to the HS:LS = 1:1 form is observed around 153 K, followed by the transformation to the pure HS state in the region 200–218 K.

The above results have thus established the existence of a thermally controlled high-spin ($S = 2$) ⇌ low-spin ($S = 0$) transition in the complex $[FeL(CN)_2]\cdot H_2O$. It should be noted that the pure LS state has been obtained separately by way of transformation of the quenched-in HS form at low temperatures. The reversible spin-state transition has thus been established only

(1) (a) Institut für Physikalische und Theoretische Chemie, University of Erlangen-Nürnberg. (b) Physikalisches Institut, Abt. II, University of Erlangen-Nürnberg.
(2) Deceased. The Queen's University of Belfast.
(3) Nelson, S. M.; McIlroy, P. D. A.; Stevenson, C. S.; König, E.; Ritter, G.; Waigel, J. *J. Chem. Soc., Dalton Trans.* **1986**, 991.

0020-1669/87/1326-3582$01.50/0

between the pure HS state above ca. 225 K and the HS:LS = 1:1 form below ca. 210 K. The present investigation has been initiated in order to clarify the unusual nature of this transition more completely.

Experimental Section

Sample Preparation. The complex $[FeL(CN)_2]\cdot H_2O$ was prepared by template synthesis following a method previously described.[3] 2,6-Diacetylpyridine was reacted with 3,6-dioxaoctane-1,8-diamine on an iron(II) template to form, as condensation product, the 15-membered N_3O_2 macrocyclic Schiff-base ligand L. A sample containing the isotope ^{57}Fe in natural abundance was employed to study general properties of the spin-state transition. A separate sample enriched in ^{57}Fe was used for the kinetic studies, in order to achieve a reasonably short time of Mössbauer-effect measurements. This sample was prepared as above by utilizing iron metal powder enriched to >90% by the isotope ^{57}Fe. The samples gave satisfactory analyses for C, H, N, and Fe. The general composition for $[FeL(CN)_2]\cdot H_2O$ is $C_{17}H_{21}N_5O_2Fe\cdot H_2O$, molecular weight 401.25. The purity of the samples was checked moreover by magnetic and Mössbauer-effect measurements. The enriched sample contained a small amount of an unidentified impurity, for which suitable corrections were applied to the measured data.

Physical Measurements. ^{57}Fe Mössbauer spectra were measured with a spectrometer consisting of a constant-acceleration electromechanical drive and a Nuclear Data ND 2400 multichannel analyzer operating in the multiscaling mode. The source used consisted of 30 mCi of ^{57}Co in rhodium at room temperature, the calibration being effected with a 25-μm iron-foil absorber. All velocity scales and isomer shifts are referred to the iron standard at 298 K. For conversion to the sodium nitroprusside scale, add +0.257 mm s^{-1}. Variable-temperature measurements between 80 and 300 K were performed by using a custom-made cryostat, the temperature being monitored by means of a calibrated iron vs. constantan thermocouple and a cryogenic temperature controller (Thor Cryogenics Model E 3010-II). The temperature stability was about ±0.10 K. Measurements at 4.2 K were performed by using a helium cryostat, applied magnetic fields being generated by a superconducting coil capable of producing 60 kG. The Mössbauer spectra were corrected for nonresonant background of the γ-rays and, for the nonenriched sample, least-squares fitted to Lorentzian line shape. For the sample enriched to >90% ^{57}Fe, a high saturation is expected and, therefore, the experimental data were fitted in terms of the general expression for the Mössbauer spectrum,[4] a correction being applied for the contribution due to a slight impurity.

In either case, the numerical procedure yields values of the effective thickness t_i, line position E_i, and line width Γ_i for each individual Mössbauer line, i. The effective thickness for the quadrupole doublets of the two phases HS and LS may then be written

$$t_{HS} = (t_1 + t_2)_{HS} = dn_{HS}f_{HS} \qquad t_{LS} = (t_1 + t_2)_{LS} = d(1 - n_{HS})f_{LS} \quad (1)$$

In eq 1, $d = N\beta\delta\sigma_0$, where N is the number of iron atoms per unit volume, β the isotopic abundance, δ the absorber thickness, and σ_0 the resonance cross section. In addition, n_{HS} is the HS fraction, f_{HS} and f_{LS} being the Debye–Waller factors of the two phases. From the above equation, the HS fraction results as

$$n_{HS} = t_{HS}/(t_{HS} + t_{LS}f_{HS}/f_{LS}) \quad (2)$$

Measurements of X-ray powder diffraction at variable temperatures were obtained with a Siemens counter diffractometer equipped with an Oxford Instruments CF 108 A flow cryostat and liquid nitrogen as coolant. The diffractometer was used in the mode of step scanning, the angular steps being 0.02 or 0.005° in terms of 2θ. Cu Kα radiation was used. The achieved temperature stability was ±0.1 K. The resulting pulses were stored in an Elscint MEDA 10 multichannel analyzer and the lines fitted to Gaussian line shape.

Results

^{57}Fe Mössbauer Effect. General Properties of the Quintet ⇌ Singlet Spin Transition. The ^{57}Fe Mössbauer effect of $[FeL(CN)_2]\cdot H_2O$ shows at 250 K a single quadrupole doublet characterized by the quadrupole splitting $\Delta E_Q = 3.218 \pm 0.003$ mm s^{-1} and the isomer shift $\delta^{IS} = +0.867 \pm 0.002$ mm s^{-1} (cf. Figure 1). Thus the thermodynamically stable form of the complex at 250 K and above is high spin (HS, $S = 2$). If the temperature is lowered slowly, a second doublet appears at about 210 K between the two HS lines. At 200 K, the Mössbauer parameters of this doublet are $\Delta E_Q = 1.344 \pm 0.008$ mm s^{-1} and $\delta^{IS} = +0.238 \pm 0.004$ mm s^{-1}. These values show that the doublet is due to the low-spin (LS, $S = 0$) ground state of the complex. At 195 K, the two doublets are comparable in intensity, the relative effective thickness assuming the value $t_{HS}/t_{tot} = 0.458$. No further change of the spectrum has been observed down to 80 K as shown in Figure 1, and no further decrease of t_{HS}/t_{tot} could be detected even after several days. If the temperature of the sample is subsequently increased, the intensity of the LS lines starts to decrease from about 225 K on, the Mössbauer spectrum assuming the character of the pure HS state at about 230 K. These observations are characterized in Figure 2 by the quantity t_{HS}/t_{tot}, which is plotted as a function of temperature. This quantity approximately represents the behavior of the HS fraction n_{HS} since, according to eq 2, $t_{HS}/t_{tot} = n_{HS}$ if the Debye–Waller factors for the two states involved, HS and LS, are identical. For slow cooling and heating, therefore, the observed transition takes place between the pure HS state at high temperature and a state consisting of HS and LS molecules in approximately equal proportion at low temperature. Evidently, the transition is associated with a pronounced hysteresis of $\Delta T_c = 15$ K, the transition temperatures determined from the center of the corresponding change being $T_c^{\uparrow} = 222$ K and $T_c^{\downarrow} = 207$ K. Detailed values of Mössbauer parameters that

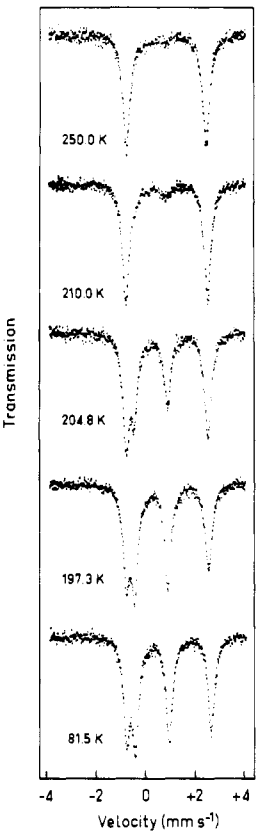

Figure 1. ^{57}Fe Mössbauer spectra of $[FeL(CN)_2]\cdot H_2O$ for slowly decreasing temperature at 250.0, 210.0, 204.8, 197.3, and 81.5 K.

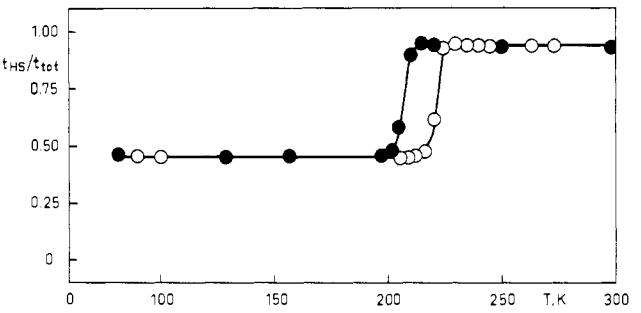

Figure 2. Temperature dependence of t_{HS}/t_{tot} for slowly decreasing (●) and increasing (○) temperature. The transition temperatures are $T_c^{\downarrow} = 207$ K and $T_c^{\uparrow} = 222$ K.

(4) König, E. Ritter, G.; Waigel, J.; Goodwin, H. A. *J. Chem. Phys.* **1985**, *83*, 3055.

Table I. ^{57}Fe Mössbauer-Effect Parameters for Slow Cooling and Heating[a]

T, K	ΔE_Q^{HS},[b] mm s^{-1}	δ^{IS}_{HS},[c] mm s^{-1}	ΔE_Q^{LS},[b] mm s^{-1}	δ^{IS}_{LS},[c] mm s^{-1}	t_{HS}/t_{tot}
250.0	3.219	+0.867			~1.0
220.2	3.288	+0.881	1.229 ± 0.053	+0.175 ± 0.026	0.938
210.0	3.320	+0.894	1.245 ± 0.024	+0.210 ± 0.012	0.897
204.8	3.320	+0.896	1.340 ± 0.007	+0.238	0.584
201.6	3.322 ± 0.007	+0.897	1.342 ± 0.008	+0.238	0.482
197.3	3.341	+0.899	1.346	+0.239	0.458
156.7	3.391	+0.924	1.345	+0.261	0.457
81.5	3.439	+0.948	1.367	+0.269	0.467
100.3	3.439	+0.946	1.358	+0.274	0.453
208.4	3.303 ± 0.009	+0.892	1.343 ± 0.008	+0.231	0.450
216.3	3.281	+0.880	1.341	+0.228	0.480
220.3	3.288	+0.881	1.337 ± 0.007	+0.224	0.617
224.3	3.295	+0.884	1.305 ± 0.024	+0.255 ± 0.012	0.926
234.9	3.261	+0.874	1.212 ± 0.034	+0.222 ± 0.017	0.942
245.0	3.242	+0.877	1.138 ± 0.036	+0.197 ± 0.018	0.938
273.0	3.180	+0.858			~1.0

[a] The data refer to the nonenriched sample of the compound and are listed in the order of measurement. [b] Experimental uncertainty smaller or equal to ±0.005 mm s^{-1} except where stated. [c] Isomer shifts δ^{IS} are listed relative to natural iron at 298 K; experimental uncertainty ±0.005 mm s^{-1} except where stated.

are assumed in the course of the transition are listed in Table I.

Similar measurements on the enriched sample of the compound show essentially the same behavior, although slight differences are apparent. Thus, the hysteresis loop for the transition between the pure HS state and the HS:LS = 1:1 form appears less abrupt and is of lower width ($T_c^{\uparrow}$ = 220.5, $T_c^{\downarrow}$ = 207, ΔT_c = 13.5 K) and the residual HS fraction at 80 K is higher (t_{HS}/t_{tot} = 0.18). On the other hand, the Mössbauer parameters for the two states, HS and LS, are practically identical with those of the nonenriched sample of $[FeL(CN)_2]\cdot H_2O$.

Irreversible Quintet (HS) → Singlet (LS) Transformation below ~160 K. If the lowering of the sample temperature from about 250 K into the region 160–180 K is reasonably fast, i.e. at about 10–20 K min^{-1}, first the HS form is retained, but this transforms, after a period of incubation, quickly into the HS:LS = 1:1 form, thus producing the value t_{HS}/t_{tot} = 0.455 in the same way as above; this value is not changed if the cooling is continued slowly down to 135 K (for clarity of presentation, these results have not been included in Figure 4). However, if the fast cooling extends into the region 150–160 K, a significantly larger LS fraction is obtained from the initial HS form, and the lower the final temperature, the larger this LS fraction. The transformation of the HS form is always irreversible and fast and below ~150 K almost complete as specified by t_{HS}/t_{tot} = 0.065, which value is maintained even if the temperature is further diminished to 80 K. As demonstrated by Figure 3, a subsequent increase of temperature produces a decrease of the LS fraction from about 150 K on, until at about 160 K, t_{HS}/t_{tot} = 0.455 again is obtained. With further increase of temperature, the increasing temperature branch of Figure 2 is followed. The transition between the pure LS state and the HS:LS = 1:1 form is centered at T_c = 157 K. A schematic diagram showing the temperature function of t_{HS}/t_{tot} for these processes is presented in Figure 4.

Quintet (HS) → Singlet (LS) Relaxation Starting from Quenched-in Quintet State. If the sample is rapidly quenched in liquid nitrogen, whereby the sample temperature drops from e.g. 310 to 77 K within a few seconds, the HS state may be "frozen in" and a transition to the LS state is not observed even within days. If the sample is now slowly warmed up, the transformation HS → LS sets in, with an observable rate, at about 100 K and becomes faster, the higher the temperature. The value finally achieved for the effective thickness is t_{HS}/t_{tot} = 0.025, i.e. smaller than the value for direct cooling from ambient temperature. Subsequent cooling to 77 K or warming to 220 K does not produce any differences from the behavior described above. A schematic diagram of t_{HS}/t_{tot} for these processes is displayed in Figure 5. The results of a kinetic study of the HS → LS transformation are reported below.

Temperature Dependence of Quadrupole Splitting and Isomer Shift. There is a pronounced temperature dependence of the

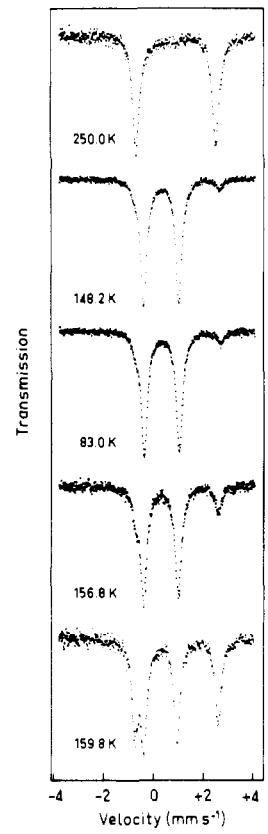

Figure 3. ^{57}Fe Mössbauer spectra of $[FeL(CN)_2]\cdot H_2O$ for reasonably fast decrease of temperature (10–20 K min^{-1}) from 250.0 to 148.2 and 83.0 K and subsequent increase of temperature to 156.8 and 159.8 K.

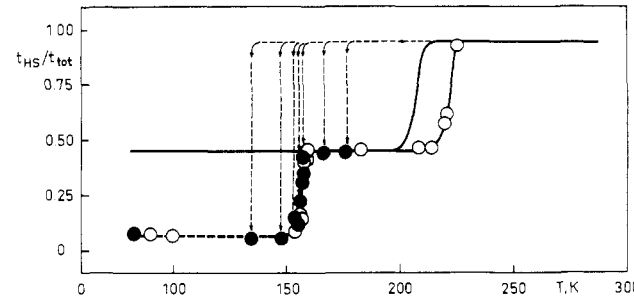

Figure 4. Schematic diagram of the temperature dependence of t_{HS}/t_{tot} for reasonably fast decrease of temperature (10–20 K min^{-1}) from 250.0 K into the region between 176.5 and 134.8 K (●) and subsequent increase of temperature (○). The transition temperature is T_c = 157 K.

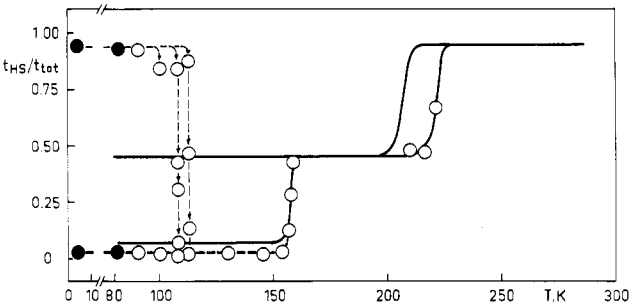

Figure 5. Schematic diagram of the temperature dependence of t_{HS}/t_{tot} for a sample quenched in liquid nitrogen.

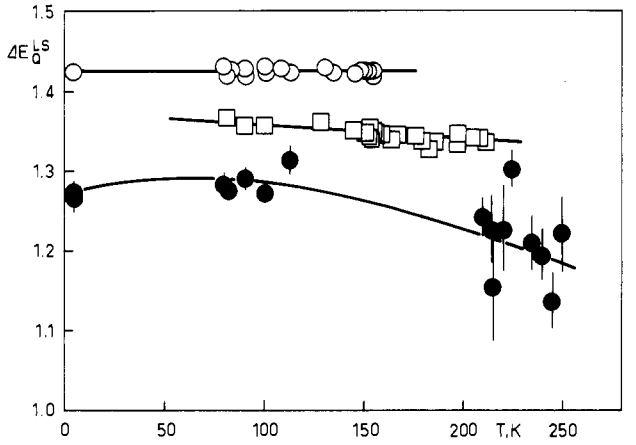

Figure 6. Temperature dependence of quadrupole splitting of the LS state ΔE_Q^{LS} for t_{HS}/t_{tot} = 0.94 (●), 0.45 (□), and 0.05 (○). Curves are drawn by inspection. The experimental uncertainty is smaller than the point size except where indicated.

quadrupole splitting for the HS state ΔE_Q^{HS} of the complex (cf. Table I) which is typical for an orbital singlet ground state as it is formed by splitting of the $^5T_2(t_2^4e^2)$ state in a ligand field of O_h symmetry. Indeed, we have verified that the temperature function of ΔE_Q^{HS} may be reasonably well fitted on the basis of the model of Ingalls,[5] although a unique set of parameter values is difficult to specify. The general consistency with this model demonstrates that the observed temperature dependence is in no way unusual.

A completely different behavior is encountered for the quadrupole splitting of the LS state, ΔE_Q^{LS}. In order to illustrate this relationship, Figure 6 shows the temperature dependence of the quantity ΔE_Q^{LS} for the three available values of t_{HS}/t_{tot} = 0.94, 0.45, and 0.05, which values have been extracted from the results of the preceding section. Evidently, the value of ΔE_Q^{LS} increases, at the same temperature, with decreasing values of t_{HS}/t_{tot}, i.e. with decreasing n_{HS}. The lower the value of n_{HS}, the lesser the dependence of ΔE_Q^{LS} on temperature. In Figure 7, we have therefore displayed ΔE_Q^{LS} as a function of t_{HS}/t_{tot} for all measurements on the unenriched sample of $[FeL(CN)_2]\cdot H_2O$. The lower curve clearly establishes that ΔE_Q^{LS} increases in two steps from about 1.25 mm s^{-1} for t_{HS}/t_{tot} = 0.95 to 1.43 mm s^{-1} for t_{HS}/t_{tot} = 0. This corresponds to a total increase of 14.5%, which is extremely unusual for the quadrupole splitting of a LS state.[6] The upper curve connecting the values 1.25 and 1.43 mm s^{-1} of ΔE_Q^{LS} results from time-dependent measurements performed subsequent to quenching of the same sample to 77 K. Similar results have been obtained for the sample of the compound enriched in ^{57}Fe.

A careful inspection of the isomer shift values δ^{IS} for the two spin states of the compound (cf. Table I) likewise reveals significant differences. Thus the isomer shift of the HS state δ^{IS}_{HS} shows a marked dependence on temperature. A linear fit of the

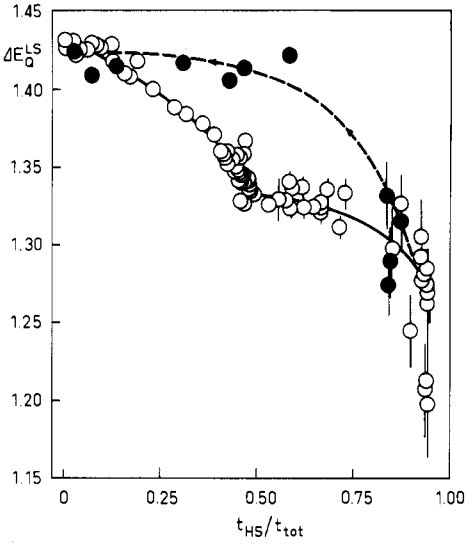

Figure 7. Quadrupole splitting of the LS state ΔE_Q^{LS} as a function of t_{HS}/t_{tot}. Curves are drawn by inspection. Arrows indicate the direction of temperature variation for time-dependent measurements (●), the results of time-independent measurements being marked (○). The experimental uncertainty is smaller than the point size except where indicated.

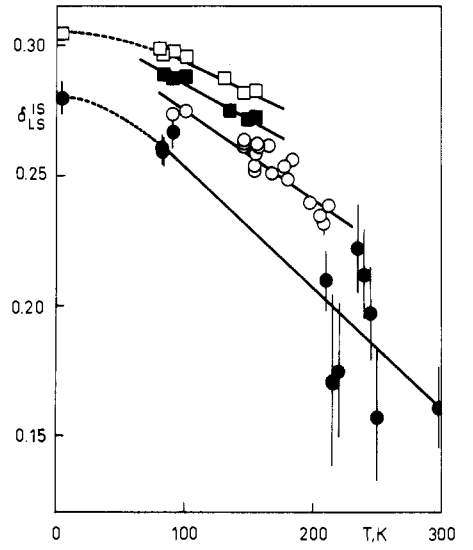

Figure 8. Temperature dependence of the isomer shift of the LS state δ^{IS}_{LS} for t_{HS}/t_{tot} = 0.94 (●), 0.45 (○), 0.07 (■), and 0.03 (□). Curves are drawn by inspection. Full straight lines are the result of linear fits.

data between 273 and 81.5 K yields the slope $\partial(\delta^{IS}_{HS})/\partial T = -(5.17 \pm 0.04) \times 10^{-4}$ mm s^{-1} K^{-1} for the unenriched sample and a closely similar result for the sample enriched in ^{57}Fe. This temperature dependence arises from the second-order Doppler effect.

Whereas there is no perceptible influence of t_{HS}/t_{tot} on the values of δ^{IS}_{HS}, such an effect may be easily demonstrated for the isomer shift of the LS state δ^{IS}_{LS}. This is illustrated in Figure 8 for the values of t_{HS}/t_{tot} = 0.03, 0.07, 0.45, and 0.94. It may be easily seen that, similar to the case for the quadrupole splitting considered above, the value of δ^{IS}_{LS} increases with decreasing values of t_{HS}/t_{tot}. Again this observation is corroborated by the analogous results for the enriched sample of the compound.

Temperature Dependence of Quantities Related to Mössbauer-Effect Areas. Line Widths and Debye–Waller Factors. All measured Mössbauer spectra show an increase in absorber line width as compared to the natural line width Γ_0 = 0.097 mm s^{-1}. In a representative spectrum, the line width of a HS doublet has been determined as Γ_{HS} = 0.163 ± 0.002 mm s^{-1}, which is 1.4 times more than the line width of a sodium nitroprusside absorber measured simultaneously. A diagrammatic disposition of the measured values as a function of temperature shows that

(5) Ingalls, R. *Phys. Rev. A* **1964**, *133*, 787.
(6) König, E.; Ritter, G.; Kulshreshtha, S. K. *Inorg. Chem.* **1984**, *23*, 1144.

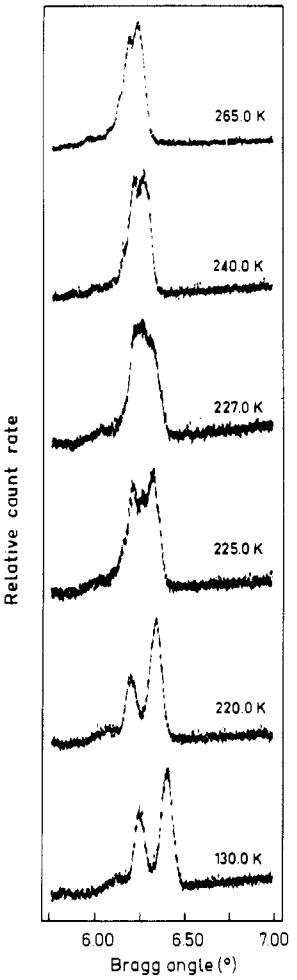

Figure 9. X-ray powder diffraction within the range $5.75° < \theta < 7°$ for slow heating between 130 and 265 K.

the line widths for HS and LS doublets are almost the same and practically independent of temperature. These results have been accounted for in the numerical fits of the spectra by assuming that the line broadening is due to a statistical distribution of ^{57}Fe nuclei about the nominal position.

According to the high-temperature approximation for the Debye–Waller factor, a linear relation between $-\ln f$ and the temperature is expected. For the present case of a spin-state transition, this dependence should hold for $-\ln t_{HS}$ if $t_{HS}/t_{tot} \simeq 1$ and for $-\ln t_{LS}$ if $t_{HS}/t_{tot} \simeq 0$. This relation has been indeed established for $-\ln t_{HS}$ and $-\ln t_{LS}$ in the region where $t_{HS}/t_{tot} = 0.95$ and 0.03, respectively. At 100 K, the resulting f factors have been obtained as $f_{HS} = 0.54$ and $f_{LS} = 0.63$. It should be noted, however, that these values are changing in the course of the measurements, the reason being the cracking of crystallites due to temperature cycling.[7] Therefore, values of n_{HS} have not been determined on the basis of eq 2, but rather values of t_{HS}/t_{tot} have been generally employed.

Measurements in External Magnetic Fields. At 4.2 K, the LS spectrum in a longitudinal magnetic field of 30 kG is modified in that the low-velocity line is split into three and the high-velocity line into two components. According to Collins and Travis,[8] this result determines the sign of the z component of the efg tensor as sgn $(V_{zz}) = +1$. A detailed numerical simulation shows moreover that, in good approximation, the asymmetry parameter $\eta = 0$. Since the HS state may be quenched in at 4.2 K (cf. Figure 5), the magnetically disturbed Mössbauer spectra for this state have also been measured. The spectra show clearly that for the HS state it is again sgn $(V_{zz}) = +1$.

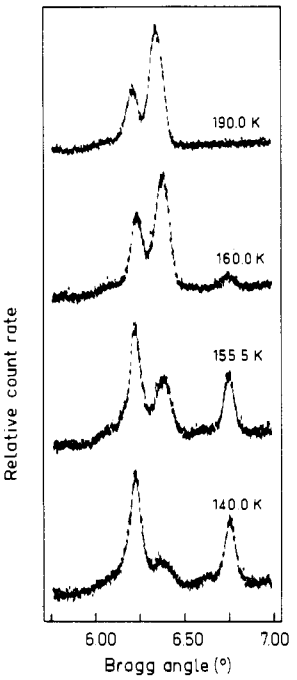

Figure 10. X-ray powder diffraction within the range $5.75° < \theta < 7°$ for slow heating between 140 and 190 K following reasonably fast cooling to 140 K.

X-ray Powder Diffraction. High-resolution X-ray diffraction of powder samples has been measured for the nonenriched sample of the compound. Figure 9 shows the peak profiles within the range $5.75° < \theta < 7°$ for slow heating between 130 and 265 K. Evidently, the diffraction pattern at 130 K is characteristic for the HS:LS = 1:1 form and that obtained at 265 K for the pure HS form. In the intermediate temperature range, the intensity of the lines originating from the HS:LS = 1:1 form is gradually decreasing while that of the HS state is increasing at the same rate. For the cooling process, the changes occur in the opposite order and at a lower transition temperature, thus confirming that hysteresis effects are present in X-ray diffraction. It has been verified that the center of the changes is approximately at the transition temperatures specified above, viz. $T_c^{\uparrow} \simeq 222$ K and $T_c^{\downarrow} \simeq 207$ K. A detailed numerical analysis of the results was unsuccessful due to the high overlap of the two patterns.

The peak profiles for increasing temperatures from 140 to 160 K, following fast cooling from ambient temperature to 140 K, are displayed in Figure 10. The initial pattern at 140 K is clearly due to the pure LS state, the resulting peaks at 190 K representing the HS:LS = 1:1 state. In the intermediate region, the transformation between the two diffraction patterns is observed. In this case, the intensity of the line at 6.75° that is characteristic for the pure LS state is seen to decrease to zero in the region of the transition temperature $T_c \simeq 157$ K.

Kinetic Study of Quintet (HS) → Singlet (LS) Relaxation between 115 and 130 K. The HS state of $[FeL(CN)_2]\cdot H_2O$ may be frozen in if the compound is quenched from ambient temperature to 77 K. The relaxation rate for the solid-state HS → LS transformation has been measured between 115.7 and 130.0 K by the ^{57}Fe Mössbauer effect. If the transformation is of second order, the rate law will be given by

$$kt = \frac{1}{t_{HS} - t_{HS}^{\infty}} - \frac{1}{t_{HS}^{0}} \qquad (3)$$

Here, t_{HS}^{0} and t_{HS}^{∞} are the initial and final values of t_{HS}, respectively, and t is the time and k the rate constant for the process. As a consequence of the definition of the effective thickness t_{HS} (cf. eq 1), the above relation reflects the behavior of the site fraction n_{HS}. The spectrum of the enriched sample was collected at regular time intervals of 40 or 50 min at the temperatures of

(7) Viegers, M. P. A.; Trooster, J. M. *Phys. Rev. B: Solid State* **1977**, *15*, 72.
(8) Collins, R.; Travis, J. *Mössbauer Eff. Methodol.* **1967**, *3*, 123.

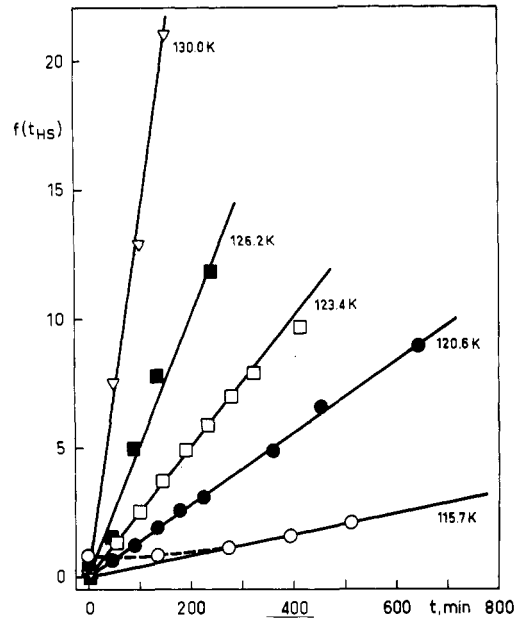

Figure 11. Dependence of $f(t_{HS}) = 1/(t_{HS} - t_{HS}^{\infty}) - 1/t_{HS}^{0}$ on time t for the irreversible HS → LS transformation at 115.7, 120.6, 123.4, 126.2, and 130.0 K following rapid quenching to 77 K.

Table II. Rate Constants for the HS → LS Relaxation in $[FeL(CN)_2]\cdot H_2O$ in the Temperature Range 115–130 K

T, K	10^5k, s^{-1}	T, K	10^5k, s^{-1}
115.7	6.77	126.2	82.75
120.6	23.18	130.0	230.8
123.4	41.80		

115.7, 120.6, 123.4, 126.2, and 130.0 K. The results are displayed in Figure 11, where the quantity $[1/(t_{HS} - t_{HS}^{\infty}) - 1/t_{HS}^{0}]$ is plotted as a function of time, t. The values of t in Figure 11 have been taken at the starting point of the time interval required for the measurement. The resulting linear plots are evidence for the applicability of eq 3, the slopes giving values of k for the temperatures employed. The values of the rate constants k have been collected in Table II. It has been observed that the transformation sets in after a certain period of incubation, which causes a deviation of the initial data from linearity. The rate law of eq 4 takes

$$k(t - t_0) = \left[\frac{1}{(t_{HS} - t_{HS}^{\infty})^2} - \frac{1}{(t_{HS}^{0})^2}\right]^{1/2} \quad (4)$$

account of this situation, as indicated by the dashed curve in Figure 11. However, this law is difficult to test for the higher temperatures since, due to the high transformation rate, data for values of t that are small as compared to the time required for the measurement could not be obtained, whereas for large values of t, the functional behavior of eq 4 is closely similar to that of eq 3. Rate laws of exponential type, such as first-order kinetics or the Avrami equation[9] $t_{HS} = 1 - \exp(-kt^n)$ for various values of n, do not provide satisfactory fits to the available data. Figure 12 shows the Arrhenius plots determined by eq 5, which were

$$\ln k = -\frac{\Delta E}{kT} + \ln A \quad (5)$$

obtained from the data of Table II as well as from the corresponding data based on eq 4. The activation energy of the transformation follows therefrom as $\Delta E = 7.3 \pm 0.4$ kcal mol^{-1} and the frequency factor as $A = 3.7 \times 10^9$ s^{-1} if the rate law of eq 3 is assumed. The relation between A and the activation entropy S^* (cf. eq 6) provides moreover the result $S^* = -4.8$ cal

$$A = (2.058 \times 10^{10})Te^{S^*/R} \quad (6)$$

(9) Rao, C. N. R.; Rao, K. J. *Phase Transitions in Solids*; McGraw-Hill: New York, 1978.

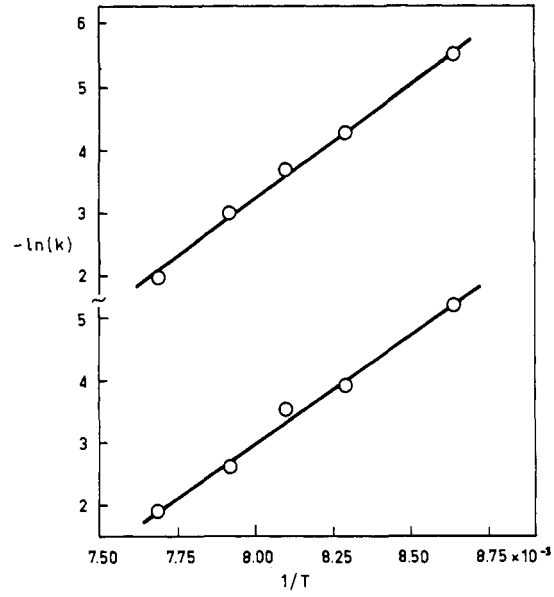

Figure 12. Arrhenius plots for irreversible HS → LS transformation following rapid quenching to 77 K according to the rate law eq 3 (upper line) and rate law eq 4 (lower line).

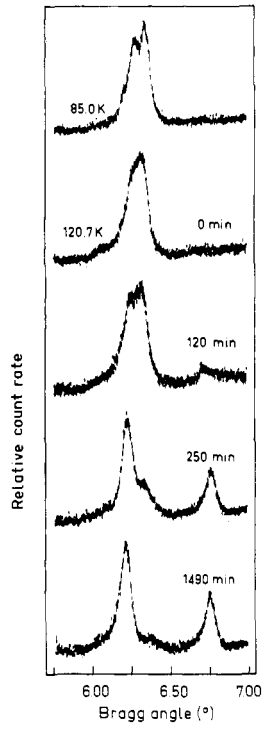

Figure 13. X-ray powder diffraction within the range $5.75° < \theta < 7°$ for the irreversible HS → LS transformation at 120.7 K as a function of time, following rapid quenching to 85 K.

K^{-1} mol^{-1} for the temperature $T = 115.7$ K, which value is well within the expected range. The corresponding results for the rate law eq 4 are $\Delta E = 6.9 \pm 0.6$ kcal mol^{-1} and $A = 8.0 \times 10^9$ s^{-1}. It should be noted that, even under the assumption of first-order kinetics or an Avrami rate law with $n = 3$, the resulting activation energy, viz. $\Delta E = 5.3$ or 5.5 kcal mol^{-1}, respectively, is not much different from the results obtained above.

In Figure 13, the time dependence of X-ray diffraction peak profiles within the range $5.75° < \theta < 7°$ is shown for the HS → LS transformation at the temperature of 120.7 K. Comparison with Figures 9 and 10 demonstrates that a HS:LS = 1:1 species similar to that found on slow cooling from ambient temperature is not formed. The transformation proceeds rather at the indicated temperature from the frozen-in HS state to the pure LS state by direct relaxation.

Discussion

The observation of a pronounced thermal hysteresis for the spin-state transition between the pure HS and the HS:LS = 1:1 state around T_c = 214.5 K shows that the transition is thermodynamically first order. This conclusion is supported by the results of X-ray powder diffraction measurements, which show that the diffraction pattern of the HS state is replaced, in the course of the transition, by a pattern characteristic for the HS:LS = 1:1 form and vice versa. No hysteresis effects were observed for the transformation of the pure LS state obtained on fast cooling to the HS:LS = 1:1 form, which is centered around 157 K. In X-ray diffraction, the powder pattern of the pure LS state is replaced by that of the HS:LS = 1:1 state as the transformation progresses. On the basis of X-ray diffraction studies of numerous spin-state-transition compounds,[10,11] the transformation may be considered likewise as thermodynamically first order. The same type of change of the powder diffraction pattern is observed for the relaxation from the frozen-in HS state to the pure LS state in the temperature region 115–130 K. This transformation may be therefore also considered as first order. It has been pointed out before[3] that for the d^6 configuration a spin singlet ground state is precluded in D_{5h} symmetry. Similar to the case for certain LS $[FeL(CN)_2]\cdot xH_2O$ complexes with other macrocyclic ligands,[3] the molecular structure of the LS form is expected to be six-coordinate with one ether oxygen of the N_3O_2 ligand remaining uncoordinated. The change of X-ray powder diffraction pattern in the course of the three transformations demonstrates that the unit cell dimensions of the HS state and of the HS:LS = 1:1 form are different from that of the LS state. As far as the molecular structure of the two forms is concerned, only speculations are possible, since X-ray structure determinations are unavailable. These forms may show a six-coordinated structure similar to that of the LS state, albeit with different metal–ligand distances and angles,[11] or a seven-coordinate pentagonal-bipyramidal structure as in the complex $[MnL(NCS)_2]$ with the same macrocyclic ligand L.[12] It should be noted that the structure of the LS complexes of type $[FeL(CN)_2]\cdot xH_2O$ with N_5 macrocycles[3] is in contrast to all previously determined structures[13-16] of metal complexes with N_5 macrocycles and also differs from the structure of the manganese(II) complex[12] with the N_3O_2 macrocyclic ligand in the complex under study. A major change of molecular structure, as that from six- to seven-coordinate, would be unusual in the solid. However, such modification of structure would be consistent with the "freezing-in" of the HS form on quenching and its transformation to the LS form on subsequent heating as well as with the direct transformation from HS to a specific fraction of HS and LS on rapid cooling from ambient temperature to below 160 K. It may be easily visualized that the lattice strain effective on the coordination unit of the metal and donor atoms on cooling would be partly alleviated if one ether oxygen atom of the flexible saturated polymethylene dioxa ligand segment would move to an unattached position. The change of molecular structure would be assisted by the gain in crystal field stabilization energy (CFSE), which is presumably responsible for the adoption of the six-coordinate structure in LS $[FeL(CN)_2]\cdot xH_2O$ complexes at low temperature. Moreover, the strain generated by the reduction of cell volume on cooling may be sufficiently counterbalanced if about 50% of the molecules adopt the LS six-coordinate form, thus forming the intermediate HS:LS = 1:1 state. A result that would be difficult to understand otherwise is the pronounced dependence of ΔE_Q^{LS} on t_{HS}/t_{tot} and thus on the HS fraction, n_{HS} (cf. Figure 7). For ions like LS iron(II) with the filled electron subshell t_{2g}^6, the crystal field contribution to the field gradient that arises from d-orbital imbalance is zero. The quadrupole splitting ΔE_Q^{LS} is therefore purely a function of the nature and distribution of ligand bonds, a fact used in the notion of partial quadrupole splitting.[17] For the LS molecules of the studied $[FeL(CN)_2]\cdot H_2O$ complex, therefore, the nature and/or distribution of ligand bonds should change as a function of the number of HS, or equally LS, molecules within the solid. The space-filling requirements of the seven-coordinate HS structure of $[FeL(CN)_2]\cdot H_2O$ and the six-coordinate LS structure of that molecule may be largely different. Given a nonnegligible interaction between the individual centers,[18] details of the ligand distribution of one state, e.g. the LS molecules, would be affected by the increasing fraction and the progressing growth of the nuclei of that phase. This assertion could provide a convenient explanation for the said dependence of ΔE_Q^{LS} on n_{HS}. It has been verified that such dependence of ΔE_Q^{LS} has not been encountered for any other spin-state transition studied so far.[10,19]

Another example of a two-step spin-state transition has been reported for $[Fe(2\text{-pic})_3]Cl_2\cdot C_2H_5OH$, where 2-pic = 2-picolylamine.[20] However, this particular transition is completely reversible, whereas on normal slow cooling the transition in $[FeL(CN)_2]\cdot H_2O$ reaches only the HS:LS = 1:1 form. The quenching-in of HS molecules of a compound that is involved in a spin-state transition is not particularly common. In the complex $[Fe(paptH)_2](NO_3)_2$, where paptH = 2-(2-pyridylamino)-4-(2-pyridyl)thiazole, a fraction of the HS state characterized, at 105 K, by n_{HS} = 0.39 may be frozen in by rapid cooling of the system from ambient to liquid-nitrogen temperature.[21] For this compound, the relaxation rate of the HS → LS transformation from the metastable HS state to the equilibrium composition has been studied in the temperature range 160–180 K. The resulting values of the rate constant, viz. $k = 6.92 \times 10^{-5}$ s^{-1} at 160 K, as well as of the activation energy, cf. ΔE = 7.50 kcal mol^{-1}, are comparable to the values obtained for the $[FeL(CN)_2]\cdot H_2O$ complex under study. These transformations are both irreversible, and it is not possible to assign to these any critical temperature, since such transformations are, because of kinetic factors, always functions of both time and temperature. Both $[FeL(CN)_2]\cdot H_2O$ and $[Fe(paptH)_2](NO_3)_2$ might be suitable for LIESST experiments[22] due to the very long lifetimes of the trapped HS state in the temperature range around 100 K.

It should be noted that, similar to $[FeL(CN)_2]\cdot H_2O$, the transition in $[Fe(paptH)_2](NO_3)_2$ is thermodynamically first order, since a pronounced hysteresis of ΔT_c = 34 K has been observed. A hysteresis of as large a width or one showing a value of at least ΔT_c = 15 K as for the complex $[FeL(CN)_2]\cdot H_2O$ may occur for kinetic reasons. In this case, the product phase cannot nucleate because of the existence of kinetic barriers. In general, the nucleation barriers are higher and ΔT_c greater for transitions showing a larger change of molecular volume ΔV. The large value of ΔV may provide a condition for the change of molecular structure between seven- and six-coordinate in the course of the spin-state transition in $[FeL(CN)_2]\cdot H_2O$. A considerable number of spin transition compounds have been investigated for nonequilibrium behavior at low temperatures,[21] although additional examples for this could not be established.

Acknowledgment. We appreciate financial support by the Deutsche Forschungsgemeinschaft, Bonn, West Germany.

Registry No. $[FeL(CN)_2]\cdot H_2O$, 103823-04-7.

(10) König, E.; Ritter, G.; Kulshreshtha, S. K. *Chem. Rev.* **1985**, *85*, 219.
(11) König, E. *Prog. Inorg. Chem.*, in press.
(12) Drew, M. G. B.; Bin Othman, A. H.; McFall, S. G.; McIlroy, P. D. A.; Nelson, S. M. *J. Chem. Soc., Dalton Trans.* **1977**, 1173.
(13) Drew, M. G. B.; Bin Othman, A. H.; Nelson, S. M. *J. Chem. Soc., Dalton Trans.* **1976**, 1394.
(14) Drew, M. G. B.; Bin Othman, A. H.; McIlroy, P.; Nelson, S. M. *Acta Crystallogr., Sect. B: Struct. Crystallogr. Cryst. Chem.* **1976**, *B32*, 1029.
(15) Drew, M. G. B.; Bin Othman, A. H.; McIlroy, P. D. A.; Nelson, S. M. *J. Chem. Soc., Dalton Trans.* **1975**, 2507.
(16) Drew, M. G. B.; Bin Othman, A. H.; McFall, S. G.; Nelson, S. M. *J. Chem. Soc., Chem. Commun.* **1975**, 818.
(17) Bancroft, G. M. *Mössbauer Spectroscopy, An Introduction for Inorganic Chemists and Geochemists*; McGraw-Hill: London, 1973.
(18) Zimmermann, R.; König, E. *J. Phys. Chem. Solids* **1977**, *38*, 779.
(19) Gütlich, P. *Struct. Bonding (Berlin)* **1981**, *44*, 83.
(20) Kaji K.; Sorai, M. *Thermochim. Acta* **1985**, *88*, 185.
(21) Ritter, G.; König, E.; Irler, W.; Goodwin, H. A. *Inorg. Chem.* **1978**, *17*, 224.
(22) Decurtins, S.; Gütlich, P.; Hasselbach, K. M.; Hauser, A.; Spiering, H. *Inorg. Chem.* **1985**, *24*, 2174.